Downlink per-user multi-streaming for FBMC/OQAM based multi-user MIMO with highly frequency selective channels

Yao Cheng, Martin Haardt
Communications Research Laboratory
Ilmenau University of Technology
P. O. Box 100565, D-98694 Ilmenau, Germany
{y.cheng, martin.haardt}@tu-ilmenau.de

Leonardo G. Baltar, Josef A. Nossek
Institute for Circuit Theory and Signal Processing
Technische Universität München
80290 Munich, Germany
{leo.baltar, josef.a.nossek}@tum.de

***Abstract*—This paper provides solutions for per-user multi-stream transmissions in FBMC/OQAM based multi-user MIMO downlink systems under highly frequency selective propagation conditions. A signal-to-leakage-plus-noise-ratio (SLNR) based metric is proposed, and it is tailored for the downlink of FBMC/OQAM based multi-user MIMO settings. Then at the base station, per-subcarrier fractionally spaced multi-tap precoders are computed based on this metric to mitigate the multi-user interference (MUI), the inter-symbol interference (ISI), as well as the inter-carrier interference (ICI) and to map the multiple data streams of each user to the transmit antennas. With the base station carrying most of the computational load, each user terminal only employs a zero-forcing (ZF) based one-tap spatial equalizer to recover the desired streams. Simulation results show that the proposed SLNR based precoding scheme achieves satisfactory performances in various multi-user MIMO downlink scenarios. It significantly outperforms the existing algorithms that require the channel on each subcarrier to be flat fading.**

I. Introduction

Filter bank based multi-carrier modulation (FBMC) has recently attracted considerable attention. As a promising alternative to orthogonal frequency division multiplexing with the cyclic prefix insertion (CP-OFDM), FBMC features a significantly reduced out-of-band radiation due to the fact that spectrally well-contained synthesis and analysis filter banks are employed at the transmitter and the receiver [1], [2]. Moreover, it is not required to insert the CP in systems where filter bank based multi-carrier with offset quadrature amplitude modulation (FBMC/OQAM) is employed, which contributes to an improved spectral efficiency compared to CP-OFDM based systems. The benefits of adopting FBMC have been demonstrated in a variety of contexts, such as asynchronous scenarios [3], [4], cognitive radio networks [5], and broadband professional mobile radio systems [6].

Most of the existing transmission schemes for FBMC/OQAM based multi-user MIMO downlink systems with space division multiple access (SDMA) have been designed based on the assumption that the channel on each subcarrier is flat fading. In case of more practical but more critical propagation conditions, e.g., if the channel exhibits severe frequency selectivity, these approaches, such as the block diagonalization (BD) based precoder in [7] and the intrinsic interference mitigating coordinated beamforming (IIM-CBF) algorithm in [8], suffer from a performance degradation.

Focusing on FBMC/OQAM with highly frequency selective channels, in [9] the authors propose linear precoders and equalizers designs based on the signal-to-leakage-plus-noise-ratio (SLNR) and on the signal to interference plus noise ratio (SINR) for a single-stream point-to-point MIMO system with the aim of maximizing the diversity gain. By considering downlink settings of FBMC/OQAM based multi-user systems also with highly frequency selective channels, the linear precoder in [10] has a structure of a filter applied on each subcarrier and its two adjacent subcarriers at twice the symbol rate. It only allows each user to have a single receive antenna. In [11], two different minimum mean square error (MMSE) based approaches have been devised for FBMC/OQAM based multi-user MISO downlink systems also considering highly frequency selective channels. A closed-form solution is provided in the first scheme, where multitap precoders and real valued equalizers are employed. While the second scheme involves a joint transmitter and receiver design via an iterative procedure to calculate the multitap precoders and equalizers. In [12] another MMSE based approach is proposed for multi-user MISO downlink FBMC/OQAM using the MSE duality from the corresponding SIMO uplink system.

In this contribution, we start with a thorough and general system model of the FBMC/OQAM based multi-user MIMO downlink setting considering highly frequency selective channels. Each user terminal is equipped with multiple receive antennas, and the transmission of multiple spatial streams to each user is enabled. A signal-to-leakage-plus-noise-ratio (SLNR) based multi-tap precoding scheme is devised to mitigate the multi-user interference (MUI), inter-symbol interference (ISI), and inter-carrier interference (ICI). Consequently, the base station with a relatively stronger computational capability is in charge of combating the interference, while at the user terminals, only single-tap zero-forcing (ZF) based receive filters are employed to recover their desired signals. Numerical simulations have been performed to evaluate the performance of the proposed SLNR based transmission strategy.

ISBN 978-3-8007-3662-1

II. System model

In the downlink setting of an FBMC/OQAM based multi-user MIMO system with M total number of subcarriers, one base station equipped with N_{T} transmit antennas serves U users simultaneously. The jth user has N_{R_j} receive antennas, whereas the total number of receive antennas of all users is denoted by $N_{\mathrm{R}} = \sum_{j=1}^{U} N_{\mathrm{R}_j}$. Multiple data streams are transmitted to each user, and d_j represents the number of data streams for the jth user. The total number of data streams is $d = \sum_{j=1}^{U} d_j$. Multi-tap precoding filters at the base station and equalizers at the user terminals are designed to mitigate the MUI, ISI, and ICI as well as to recover the desired streams. After the OQAM staggering [1], the qth data stream transmitted to the sth user on the ℓth subcarrier is denoted by $x_\ell^{s,q}[n]$, for $q = 1, 2, \ldots, d_s$, and $s = 1, 2, \ldots, U$. It has following structure

$$\begin{cases} \left[\alpha_\ell^{s,q}[m] \quad \jmath\beta_\ell^{s,q}[m] \quad \alpha_\ell^{s,q}[m-1] \quad \cdots\right]^{\mathrm{T}}, \text{ for } \ell \text{ odd}, \\ \left[\jmath\beta_\ell^{s,q}[m] \quad \alpha_\ell^{s,q}[m] \quad \jmath\beta_\ell^{s,q}[m-1] \quad \cdots\right]^{\mathrm{T}}, \text{ for } \ell \text{ even}, \end{cases}$$

where $\alpha_\ell^{s,q}[m]$ and $\beta_\ell^{s,q}[m]$ represent the real part and the imaginary part of the QAM modulated data symbol, but even so we make the common assumption that they are Gaussian distributed with unit variance and i.i.d.. Moreover, the impulse response of the precoding filter for $x_\ell^{s,q}[n]$ is given by $b_\ell^{i,s,q}[n]$, for $i = 1, 2, \ldots, N_{\mathrm{T}}$, while B denotes the length of the precoding filters. Fig. 1 illustrates this per-subcarrier precoding procedure. Then, the resulting signals are multiplexed by the synthesis filter banks (SFBs). The aforementioned transmit processing for the kth subcarrier is depicted in Fig. 2. Throughout this work, highly frequency selective channels are considered, whereas $h_{\mathrm{ch}}^{i,j,r}[l_{\mathrm{P}}]$ represents the impulse response of the propagation channel between the ith transmit antenna and the rth receiver antenna of the jth user. In our model, we also assume that the signal on the kth subcarrier is only contaminated by interference from the $(k-1)$th, the $(k+1)$th subcarrier and colored noise [11], [13]. The equivalent channel impulse response for the signal that is passed through the synthesis filter of the ℓth subcarrier, transmitted between the ith transmit antenna and the rth receive antenna of the jth user, and passed through the analysis filter for the kth subcarrier can be expressed as

$$h_{\ell,k}^{i,j,r}[n] = \left(h_\ell[l_{\mathrm{P}}] * h_{\mathrm{ch}}^{i,j,r}[l_{\mathrm{P}}] * h_k[l_{\mathrm{P}}]\right)\Big|_{l_{\mathrm{P}}=n\frac{M}{2}}, \qquad (1)$$

where $*$ represents the discrete-time convolution operation and $h_k[l_{\mathrm{P}}]$ the impulse response of the pulse shaping filter for the kth subcarrier. Here the effects of the transmit filter, the propagation channel, the receive filter as well as the upsampling and downsampling operations are included. The resulting number of taps of this equivalent channel is

$$Q = \left\lceil \frac{2(L_{\mathrm{P}}-1) + L_{\mathrm{ch}}}{M/2} \right\rceil, \qquad (2)$$

where $\lceil \bullet \rceil$ represents the ceil operation, and L_{ch} and L_{P} denote the length of the channel impulse response and the length of the prototype filter, respectively. Here, for the prototype filter we choose a root raised cosine (RRC) with roll-off one and impulse response duration length $L_{\mathrm{P}} = KM + 1$ samples[11], [13], where K represents the time overlapping factor. At the receiver, signals from the subchannels are separated by an analysis filter bank (AFB). Taking the case of the rth receive antenna of the jth user and the kth subcarrier as an example, we present the receiver block diagram in Fig. 3. For the rth receive antenna of the jth user on the kth subcarrier an equalizer is applied for each stream. The impulse response of the corresponding equalizer that recovers the pth data stream, with $p = 1, 2, \ldots, d_j$, is represented by $g_k^{j,r,p}[n]$, where $j = 1, 2, \ldots, U$, and $r = 1, 2, \ldots, N_{\mathrm{R}_j}$. The recovered pth data stream of the jth user on the kth subcarrier can be now written as

$$\hat{x}_k^{j,p}[n] = \sum_{r=1}^{N_{\mathrm{R}_j}} g_k^{j,r,p}[n] * \left(\sum_{i=1}^{N_{\mathrm{T}}} \left(\sum_{\ell=k-1}^{k+1} \left(h_{\ell,k}^{i,j,r}[n] * \sum_{s=1}^{U} \sum_{q=1}^{d_s} \left(b_\ell^{i,s,q}[n] * x_\ell^{s,q}[n] \right) \right) \right) + \hat{\eta}_k^{j,r}[n] \right), \qquad (3)$$

where $\hat{\eta}_k^{j,r}[n]$ denotes the filtered AWGN.

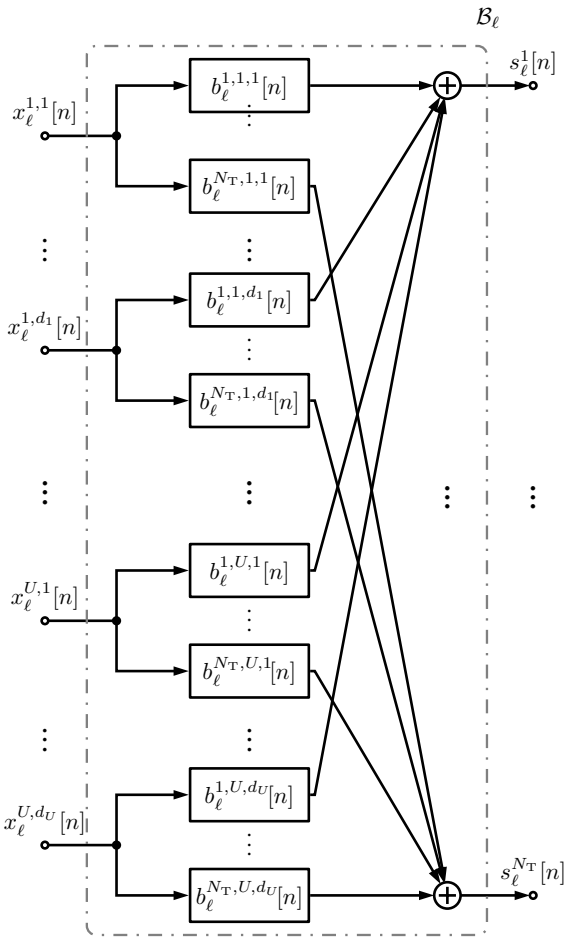

Figure 1. Precoding of multiple data streams of each of U users onto N_{T} transmit antennas for subcarrier ℓ

III. Signal-to-leakage-plus-noise-ratio (SLNR) maximization based precoder

In this section, we design signal-to-leakage-plus-noise-ratio (SLNR) based precoders to mitigate the MUI, ISI and ICI. To keep a low computational burden at each user terminal, single-tap spatial receive filters are employed, and they are assumed to be real-valued. Therefore, we can further express

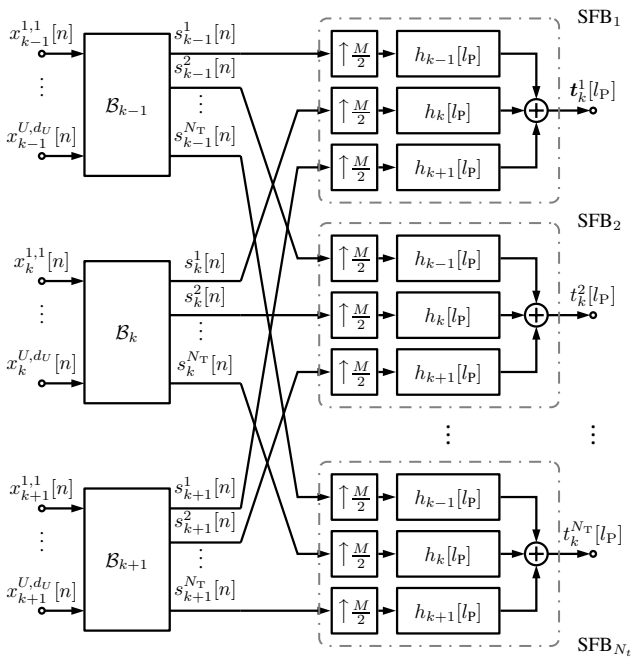

Figure 2. Transmitter model of an FBMC/OQAM based multi-user MIMO downlink system with precoding filters for the kth subcarrier

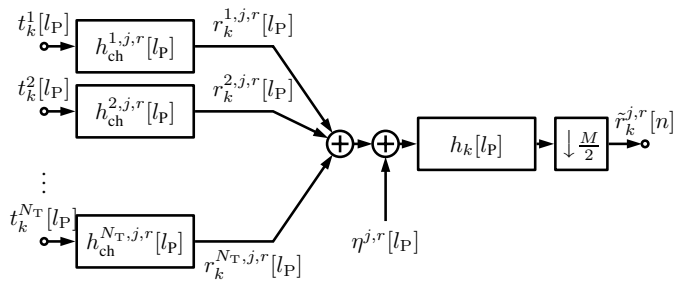

Figure 3. Receiver block diagram for the rth receive antenna of the jth user on the kth subcarrier

the recovered desired signal $\hat{\alpha}_k^{j,p}[m]$ in the following matrix-vector formulation

$$\hat{\alpha}_k^{j,p}[m] = \sum_{r=1}^{N_{\mathrm{R}_j}} g_k^{j,r,p} \cdot \mathrm{Re}\left\{ \sum_{\ell=k-1}^{k+1} \sum_{s=1}^{U} \sum_{q=1}^{d_s} \boldsymbol{x}_\ell^{s,q^\mathrm{T}}[n] \cdot \boldsymbol{H}_{\ell,k}^{j,r} \cdot \boldsymbol{b}_\ell^{s,q} + \hat{\eta}_k^{j,r}[n] \right\}, \tag{4}$$

where

$$\boldsymbol{b}_\ell^{s,q} = \begin{bmatrix} \boldsymbol{b}_\ell^{1,s,q^\mathrm{T}} & \boldsymbol{b}_\ell^{2,s,q^\mathrm{T}} & \dots & \boldsymbol{b}_\ell^{N_\mathrm{T},s,q^\mathrm{T}} \end{bmatrix}^\mathrm{T} \in \mathbb{C}^{N_\mathrm{T}\cdot B} \tag{5}$$

contains the $N_\mathrm{T} \cdot B$ coefficients of the precoding filters for the qth data stream of the sth user that is transmitted on the ℓth subcarrier, and

$$\boldsymbol{H}_{\ell,k}^{j,r} = \begin{bmatrix} \boldsymbol{H}_{\ell,k}^{1,j,r} & \boldsymbol{H}_{\ell,k}^{2,j,r} & \dots & \boldsymbol{H}_{\ell,k}^{N_\mathrm{T},j,r} \end{bmatrix} \in \mathbb{C}^{(B+Q-1)\times N_\mathrm{T}\cdot B} \tag{6}$$

where $\boldsymbol{H}_{\ell,k}^{i,j,r} \in \mathbb{C}^{(B+Q-1)\times B}$, for $i = 1, 2, \dots, N_\mathrm{T}$, is a Toeplitz matrix with the equivalent channel coefficients $h_{\ell,k}^{i,j,r}[n]$. The data vector $\boldsymbol{x}_\ell^{s,q}[n] \in \mathbb{C}^{B+Q-1}$ contains consecutive data symbols of the qth data stream of the sth user, whereas $g_k^{j,r,p}$ denotes the real-valued coefficient of the spatial filter to recover the pth data stream of the jth user on the kth subcarrier from the signals received by the rth receive antenna. When estimates of $\beta_k^{j,p}[m]$ are desired, they are obtained by taking the imaginary part of (3). Since both cases are equivalent to each other, we focus on the case of $\hat{\alpha}_k^{j,p}[m]$ in the sequel.

First, let us define the terms c_k^j and u_k^j to measure the total interference power caused by the signal of the jth user from the kth subcarrier on the adjacent subcarriers and the other users, respectively. They take the following forms

$$c_k^j = \mathrm{E}\left\{ \sum_{r=1}^{N_{\mathrm{R}_j}} \sum_{\ell=k-1,\ell\neq k}^{k+1} \sum_{q=1}^{d_j} \left| \mathrm{Im}\left\{ \boldsymbol{x}_k^{j,q^\mathrm{T}}[n] \cdot \boldsymbol{H}_{\ell,k}^{j,r} \cdot \boldsymbol{b}_k^{j,q} \right\} \right|^2 \right\}, \tag{7}$$

$$u_k^j = \mathrm{E}\left\{ \sum_{s=1,s\neq j}^{U} \sum_{r=1}^{N_{\mathrm{R}_s}} \sum_{q=1}^{d_j} \left(\sum_{\ell=k-1,\ell\neq k}^{k+1} \left| \mathrm{Im}\left\{ \boldsymbol{x}_k^{j,q^\mathrm{T}}[n] \cdot \boldsymbol{H}_{\ell,k}^{s,r} \cdot \boldsymbol{b}_k^{j,q} \right\} \right|^2 + \left| \mathrm{Re}\left\{ \boldsymbol{x}_k^{j,q^\mathrm{T}}[n] \cdot \boldsymbol{H}_{k,k}^{s,r} \cdot \boldsymbol{b}_k^{j,q} \right\} \right|^2 \right) \right\}. \tag{8}$$

We further define $\widetilde{\boldsymbol{x}}_k^{j,q}[n] \in \mathbb{R}^{B+Q-1}$ such that

$$\boldsymbol{x}_k^{j,q}[n] = \boldsymbol{J}_k \cdot \widetilde{\boldsymbol{x}}_k^{j,q}[n], \tag{9}$$

where the diagonal matrix $\boldsymbol{J}_k \in \mathbb{C}^{(B+Q-1)\times(B+Q-1)}$ has "1" and "j" alternately appearing on its diagonal. Similarly as in [11], the following linear expressions for the real part and the imaginary part of the interference terms in (7) and (8) can be obtained

$$\mathrm{Re}\left\{ \boldsymbol{x}_k^{j,q^\mathrm{T}}[n] \cdot \boldsymbol{H}_{k,k}^{s,r} \cdot \boldsymbol{b}_k^{j,q} \right\} = \widetilde{\boldsymbol{x}}_k^{j,q^\mathrm{T}}[n] \cdot \boldsymbol{\Psi}_{k,k}^{s,r} \cdot \boldsymbol{\xi}_k^{j,q} \tag{10}$$

$$\mathrm{Im}\left\{ \boldsymbol{x}_k^{j,q^\mathrm{T}}[n] \cdot \boldsymbol{H}_{\ell,k}^{s,r} \cdot \boldsymbol{b}_k^{j,q} \right\} = \widetilde{\boldsymbol{x}}_k^{j,q^\mathrm{T}}[n] \cdot \boldsymbol{\Phi}_{\ell,k}^{s,r} \cdot \boldsymbol{\xi}_k^{j,q} \tag{11}$$

where $\boldsymbol{\Psi}_{k,k}^{s,r} \in \mathbb{R}^{(B+Q-1)\times 2\cdot N_\mathrm{T}\cdot B}$, $\boldsymbol{\Phi}_{\ell,k}^{s,r} \in \mathbb{R}^{(B+Q-1)\times 2\cdot N_\mathrm{T}\cdot B}$, and $\boldsymbol{\xi}_k^{j,q} \in \mathbb{R}^{2\cdot N_\mathrm{T}\cdot B}$ are defined as

$$\boldsymbol{\Psi}_{k,k}^{s,r} = \begin{bmatrix} \mathrm{Re}\left\{ \boldsymbol{J}_k \cdot \boldsymbol{H}_{k,k}^{s,r} \right\} & -\mathrm{Im}\left\{ \boldsymbol{J}_k \cdot \boldsymbol{H}_{k,k}^{s,r} \right\} \end{bmatrix} \tag{12}$$

$$\boldsymbol{\Phi}_{\ell,k}^{s,r} = \begin{bmatrix} \mathrm{Im}\left\{ \boldsymbol{J}_k \cdot \boldsymbol{H}_{\ell,k}^{s,r} \right\} & \mathrm{Re}\left\{ \boldsymbol{J}_k \cdot \boldsymbol{H}_{\ell,k}^{s,r} \right\} \end{bmatrix} \tag{13}$$

$$\boldsymbol{\xi}_k^{j,q} = \begin{bmatrix} \mathrm{Re}\left\{ \boldsymbol{b}_k^{j,q} \right\} \\ \mathrm{Im}\left\{ \boldsymbol{b}_k^{j,q} \right\} \end{bmatrix}. \tag{14}$$

In addition, we introduce

$$\boldsymbol{\Xi}_k^j = \begin{bmatrix} \boldsymbol{\xi}_k^{j,1} & \boldsymbol{\xi}_k^{j,2} & \dots & \boldsymbol{\xi}_k^{j,d_j} \end{bmatrix} \in \mathbb{R}^{2\cdot N_\mathrm{T}\cdot B\times d_j} \tag{15}$$

for the jth user and the kth subcarrier such that the d_j columns of $\boldsymbol{\Xi}_k^j$ correspond to the precoders for the d_j data streams of the jth user that are transmitted on the kth subcarrier.

Recalling that data symbols are i.i.d., we reformulate the terms c_k^j and u_k^j as follows

$$c_k^j = \sum_{q=1}^{d_j} \boldsymbol{\xi}_k^{j,q^\mathrm{T}} \cdot \left(\sum_{r=1}^{N_{\mathrm{R}_j}} \sum_{\ell=k-1,\ell\neq k}^{k+1} \boldsymbol{\Phi}_{\ell,k}^{j,r^\mathrm{T}} \cdot \boldsymbol{\Phi}_{\ell,k}^{j,r} \right) \cdot \boldsymbol{\xi}_k^{j,q} = \mathrm{Tr}\left\{ \boldsymbol{\Xi}_k^{j^\mathrm{T}} \cdot \left(\sum_{r=1}^{N_{\mathrm{R}_j}} \sum_{\ell=k-1,\ell\neq k}^{k+1} \boldsymbol{\Phi}_{\ell,k}^{j,r^\mathrm{T}} \cdot \boldsymbol{\Phi}_{\ell,k}^{j,r} \right) \cdot \boldsymbol{\Xi}_k^j \right\}, \tag{16}$$

$$u_k^j = \sum_{q=1}^{d_j} \boldsymbol{\xi}_k^{j,q^{\mathrm{T}}} \cdot \left(\sum_{s=1,s\neq j}^{U} \sum_{r=1}^{N_{\mathrm{R}s}} \left(\sum_{\ell=k-1,\ell\neq k}^{k+1} \boldsymbol{\Phi}_{\ell,k}^{s,r^{\mathrm{T}}} \cdot \boldsymbol{\Phi}_{\ell,k}^{s,r} + \boldsymbol{\Psi}_{k,k}^{s,r^{\mathrm{T}}} \cdot \boldsymbol{\Psi}_{k,k}^{s,r} \right) \right) \cdot \boldsymbol{\xi}_k^{j,q}$$
$$= \mathrm{Tr}\left\{ \boldsymbol{\Xi}_k^{j^{\mathrm{T}}} \cdot \left(\sum_{s=1,s\neq j}^{U} \sum_{r=1}^{N_{\mathrm{R}s}} \left(\sum_{\ell=k-1,\ell\neq k}^{k+1} \boldsymbol{\Phi}_{\ell,k}^{s,r^{\mathrm{T}}} \cdot \boldsymbol{\Phi}_{\ell,k}^{s,r} + \boldsymbol{\Psi}_{k,k}^{s,r^{\mathrm{T}}} \cdot \boldsymbol{\Psi}_{k,k}^{s,r} \right) \right) \cdot \boldsymbol{\Xi}_k^{j} \right\}, \quad (17)$$

where $\mathrm{Tr}\{\cdot\}$ represents the trace of the input matrix.

Moreover, the power of the ISI added to the signal of the jth user on the kth subcarrier is measured via

$$\mathrm{ISI}_k^j = \mathrm{E}\left\{ \sum_{r=1}^{N_{\mathrm{R}_j}} \sum_{q=1}^{d_j} \left| \widetilde{\boldsymbol{x}}_k^{j,q^{\mathrm{T}}}[n] \cdot \boldsymbol{\Psi}_{k,k}^{(\mathrm{int}),j,r} \cdot \boldsymbol{\xi}_k^{j,q} \right|^2 \right\}$$
$$= \mathrm{Tr}\left\{ \boldsymbol{\Xi}_k^{j^{\mathrm{T}}} \cdot \sum_{r=1}^{N_{\mathrm{R}_j}} \boldsymbol{\Psi}_{k,k}^{(\mathrm{int}),j,r^{\mathrm{T}}} \cdot \boldsymbol{\Psi}_{k,k}^{(\mathrm{int}),j,r} \cdot \boldsymbol{\Xi}_k^{j} \right\}, \quad (18)$$

where

$$\boldsymbol{\Psi}_{k,k}^{(\mathrm{int}),j,r} = \boldsymbol{J}_{\mathrm{int}}^{(\nu)} \cdot \boldsymbol{\Psi}_{k,k}^{j,r} \in \mathbb{R}^{(B+Q-1)\times 2\cdot N_{\mathrm{T}}\cdot B}. \quad (19)$$

Here $\boldsymbol{J}_{\mathrm{int}}^{(\nu)} \in \mathbb{R}^{(B+Q-1)\times(B+Q-1)}$ is constructed by replacing the νth row of a $(B+Q-1)$-by-$(B+Q-1)$ identity matrix by an all-zeros vector, where $\nu = \lceil \frac{B+Q-1}{2} \rceil$ is the (integer) delay of the system.

The effective channel with respect to the rth receive antenna of the jth user for the kth subcarrier is given by

$$\boldsymbol{h}_{k,k}^{(\mathrm{eff}),j,r} = \boldsymbol{\Psi}_{k,k}^{j,r^{\mathrm{T}}} \cdot \boldsymbol{e}_\nu \in \mathbb{R}^{2\cdot N_{\mathrm{T}}\cdot B}, \quad (20)$$

where $\boldsymbol{e}_\nu \in \mathbb{R}^{B+Q-1}$ denotes a unit vector with its νth element as one.

Finally, the SLNR on the kth subcarrier for the jth user represented by SLNR_k^j takes the form in (21) on the next page, where $\rho = 0.5 \cdot \frac{1}{d_j} \cdot N_{\mathrm{R}_j} \cdot \gamma \cdot \sigma_n^2$, σ_n^2 represents the noise variance and γ results from the filtering and the downsampling operation as illustrated in Fig. 3. The d_j columns of $\boldsymbol{\Xi}_k^j$ are obtained as the d_j generalized eigenvectors of the pair $\{\boldsymbol{A}, \boldsymbol{C}\}$ as defined in (21) that correspond to the d_j largest generalized eigenvalues [14], [15]. Then $\boldsymbol{\Xi}_k^j$ is scaled such that $\mathrm{Tr}\left\{ \boldsymbol{\Xi}_k^{j^{\mathrm{T}}} \cdot \boldsymbol{\Xi}_k^j \right\} = d_j$ is fulfilled.

At each user terminal, assuming that the MUI, ISI, and ICI have been eliminated, $\hat{\alpha}_k^{j,p}[m]$ can be written as follows in the interference free and noiseless case

$$\hat{\alpha}_k^{j,p}[m] = \sum_{r=1}^{N_{\mathrm{R}_j}} g_k^{j,r,p} \cdot \mathrm{Re}\left\{ \sum_{q=1}^{d_s} \boldsymbol{x}_k^{j,q^{\mathrm{T}}}[n] \cdot \boldsymbol{H}_{k,k}^{j,r} \cdot \boldsymbol{b}_k^{j,q} \right\}. \quad (22)$$

The effective channel for the d_j spatial streams of the jth user on the kth subcarrier is given by $\check{\boldsymbol{H}}_{k,k}^j \in \mathbb{R}^{N_{\mathrm{R}_j}\times d_j}$, and its (r,q)th entry, for $r = 1, 2, \ldots, N_{\mathrm{R}_j}$ and $q = 1, 2, \ldots, d_j$, is written as

$$\check{h}_{k,k}^{j,r,q} = \mathrm{Re}\left\{ \boldsymbol{e}_\nu^{\mathrm{T}} \cdot \boldsymbol{H}_{k,k}^{j,r} \cdot \boldsymbol{b}_k^{j,q} \right\}. \quad (23)$$

Now define a matrix $\boldsymbol{G}_k^j \in \mathbb{R}^{N_{\mathrm{R}_j}\times d_j}$ such that it contains the coefficients of the single-tap spatial receive filter for the jth user on the kth subcarrier, i.e., $g_k^{j,r,p}$ is its (r,q)th entry, again for $r = 1, 2, \ldots, N_{\mathrm{R}_j}$ and $q = 1, 2, \ldots, d_j$. With zero-forcing (ZF) as the criterion, $\boldsymbol{G}_k^j$ can be computed as

$$\boldsymbol{G}_k^j = \check{\boldsymbol{H}}_{k,k}^j \cdot \left(\check{\boldsymbol{H}}_{k,k}^{j^{\mathrm{T}}} \cdot \check{\boldsymbol{H}}_{k,k}^j \right)^{-1}. \quad (24)$$

In this way we can compute with closed forms first the multi-tap precoders and then the spatial equalizers. It is worth noting that, although the received symbols of each user in a particular subcarrier are always dependent on the precoders of the adjacent subcarriers and of the other users, with the SLNR criterion we are able to decouple them because the precoders are designed to also minimize the interference they cause on adjacent subcarriers and on the other users.

IV. Simulation results

In this section, we evaluate the performance of the proposed transmitter and receiver designs in various multi-user MIMO downlink settings. The total number of subcarriers is M =128, whereas the number of subcarriers with data symbols is M_{u} =72. The subcarrier spacing is set to 15 kHz, and the bandwidth is 1.4 MHz. The data symbols are drawn from the 16-QAM constellation. The ITU Veh-B channel is used. The maximum channel impulse impulse length is approximately $L_{\mathrm{ch}} = 47$ samples.

A two-user scenario is considered in the first example. The base station is equipped with six transmit antennas, whereas each of the two users has three receive antennas, i.e., $U = 2$, $N_{\mathrm{T}} = 6$, and $N_{\mathrm{R}_1} = N_{\mathrm{R}_2} = 3$. Two data streams are transmitted to each user, i.e., $d_1 = d_2 = 2$. The bit error rate (BER) performance of the proposed SLNR based multi-tap precoding scheme is shown in Fig. 4. Different lengths of the precoder, i.e., different values for B, are considered. It can be observed that as the length of the precoder is longer, a better performance is achieved due to a more effective mitigation of the MUI, ISI, and ICI. Nevertheless, increasing the length of the precoder from 9 to 11 only leads to a very slight improvement for the scenario considered. With $B = 5$, the performance is already satisfactory over the range of the uncoded BER that is of interest. For the purpose of comparison, the IIM-CBF 1 scheme [8] and the BD based method [7] have also been simulated. Note that these two approaches rely on the assumption that the channel on each subcarrier is flat fading. Since this assumption is violated, and the propagation channel is highly frequency selective, they fail to effectively suppress the interference. Therefore, we can see in Fig. 4 that the proposed SLNR based precoding algorithm significantly outperforms IIM-CBF 1 and the BD based method even when $B = 3$.

In the second example, we assess the performance of the SLNR based precoder in two other multi-user MIMO downlink scenarios, and the results are presented in Fig. 5. It can be observed that the SLNR based precoding scheme leads to a

$$\mathrm{SLNR}_k^j = \frac{\mathrm{Tr}\left\{ \boldsymbol{\Xi}_k^{j^{\mathrm{T}}} \cdot \overbrace{\sum_{r=1}^{N_{\mathrm{R}_j}} \boldsymbol{h}_{k,k}^{(\mathrm{eff}),j,r} \cdot \boldsymbol{h}_{k,k}^{(\mathrm{eff}),j,r^{\mathrm{T}}}}^{\boldsymbol{A}} \cdot \boldsymbol{\Xi}_k^j \right\}}{\mathrm{Tr}\left\{ \boldsymbol{\Xi}_k^{j^{\mathrm{T}}} \cdot \underbrace{\left(\sum_{s=1}^{U} \sum_{r=1}^{N_{\mathrm{R}_s}} \sum_{\ell=k-1,\ell\neq k}^{k+1} \boldsymbol{\Phi}_{\ell,k}^{s,r^{\mathrm{T}}} \cdot \boldsymbol{\Phi}_{\ell,k}^{s,r} + \sum_{s=1,s\neq j}^{U} \sum_{r=1}^{N_{\mathrm{R}_s}} \boldsymbol{\Psi}_{k,k}^{s,r^{\mathrm{T}}} \cdot \boldsymbol{\Psi}_{k,k}^{s,r} + \sum_{r=1}^{N_{\mathrm{R}_j}} \boldsymbol{\Psi}_{k,k}^{(\mathrm{int}),j,r^{\mathrm{T}}} \cdot \boldsymbol{\Psi}_{k,k}^{(\mathrm{int}),j,r} + \rho \cdot \boldsymbol{I}_{2 \cdot N_{\mathrm{T}} \cdot B} \right)}_{\boldsymbol{C}} \cdot \boldsymbol{\Xi}_k^j \right\}} \tag{21}$$

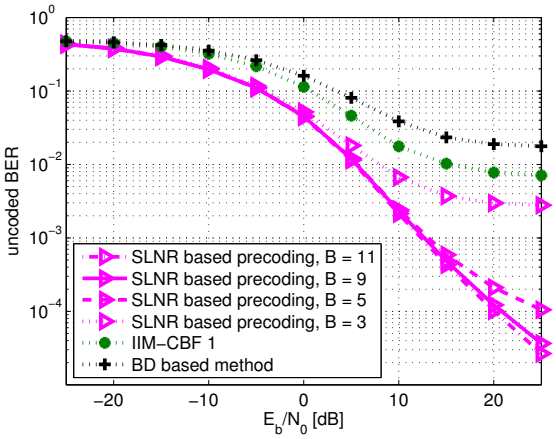

Figure 4. BER performance in multi-user MIMO downlink settings where $U = 2$, $N_{\mathrm{R}_1} = N_{\mathrm{R}_2} = 3$, $N_{\mathrm{T}} = 6$, $d_1 = d_2 = 2$

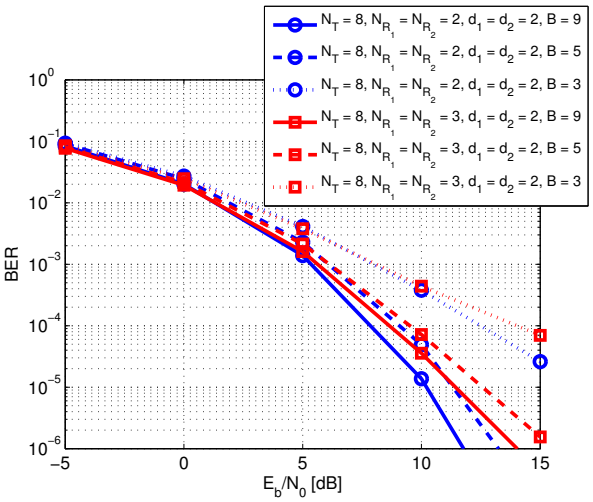

Figure 5. BER performance in multi-user MIMO downlink settings where $U = 2$, $N_{\mathrm{R}_1} = N_{\mathrm{R}_2} = 2$ or $N_{\mathrm{R}_1} = N_{\mathrm{R}_2} = 3$, $N_{\mathrm{T}} = 8$, $d_1 = d_2 = 2$

satisfactory performance in these settings, too. As the number of receive antennas of each user terminal increases, the spatial degrees of freedom that are exploited for the mitigation of the MUI are reduced. On the other hand, a larger number of receive antennas brings a higher diversity gain. As the former effect appears to dominate in the scenario tested, the BER performance in case of the $N_{\mathrm{R}_1} = N_{\mathrm{R}_2} = 2$ setting is slightly better than that of the $N_{\mathrm{R}_1} = N_{\mathrm{R}_2} = 3$ setting.

V. Conclusions

In this paper we have proposed design methods of precoders and equalizers for the downlink of multi-user MIMO FBMC/OQAM systems that enable multi-streaming when the mobile stations are equipped with multiple antennas. For the precoders design our approach is based on the maximization of the SLNR, in order to decouple the influence of precoders on adjacent subcarriers and between the users. For the spatial real-valued single-tap equalizers we have employed a zero forcing design criterion. We first design the precoders and then the equalizers, both with closed forms. The simulation results show that the algorithm is effective in combating MUI, ICI and ISI in highly frequency selective propagation conditions and also enables spatial multiplexing as desired.

Acknowledgment

The authors gratefully acknowledge the financial support by the European Union FP7-ICT project EMPhAtiC (http://www.ict-emphatic.eu) under grant agreement no. 318362.

References

[1] P. Siohan, C. Siclet, and N. Lacaille, "Analysis and design of OFDM/OQAM systems based on filterbank theory," *IEEE Transactions on Signal Processing*, vol. 50, no. 5, pp. 1170 – 1183, May 2002.

[2] M. G. Bellanger, "Specification and design of a prototype filter for filter bank based multicarrier transmission," in *Proc. IEEE Int. Conf. Acoustics, Speech, and Signal Processing*, May 2001.

[3] T. Fusco, A. Petrella, and M. Tanda, "Sensitivity of multi-user filter-bank multicarrier systems to synchronization errors," in *Proc. ISCCSP*, Mar. 2008.

[4] H. Saeedi-Sourck, Y. Wu, J. W. M. Bergmans, S. Sadri, and B. Farhang-Boroujeny, "Complexity and performance comparison of filter bank multicarrier and OFDM in uplink of multicarrier multiple access networks," *IEEE Transactions on Signal Processing*, vol. 59, no. 4, pp. 1907–1912, Apr. 2011.

[5] M. Shaat and F. Bader, "Computationally efficient power allocation algorithm in multicarrier-based cognitive radio networks: OFDM and FBMC systems," *EURASIP Journal on Advances in Signal Processing*, vol. 2010, Mar. 2010.

[6] M. Renfors, F. Bader, L. Baltar, D. Le Ruyet, D. Roviras, P. Mege, and M. Haardt, "On the use of filter bank based multicarrier modulation for professional mobile radio," in *Proc. 77th IEEE Vehicular Technology Conf. (VTC 2013 Spring)*, June 2013.

[7] M. Caus, A. I. Perez-Neira, and M. Moretti, "SDMA for FBMC with block diagonalization," in *Proc. SPAWC 2013*, June 2013.

[8] Y. Cheng, P. Li, and M. Haardt, "Intrinsic interference mitigating coordinated beamforming for the FBMC/OQAM based downlink," *EURASIP Journal on Advances in Signal Processing*, May 2014.

[9] M. Caus and A.I. Perez-Neira, "Transmitter-receiver designs for highly frequency selective channels in MIMO FBMC systems," *IEEE*

Transactions on Signal Processing, vol. 60, no. 12, pp. 6519–6532, Dec. 2012.

[10] F. Horlin, J. Fickers, T. Deleu, and J. Louveaux, "Interference-free SDMA for FBMC-OQAM," *EURASIP Journal on Advances in Signal Processing*, vol. 46, Mar. 2013.

[11] M. Newinger, L. G. Baltar, A. L. Swindlehurst, and J. A. Nossek, "MISO Broadcasting FBMC System for Highly Frequency Selective Channels," in *Proc. International ITG Workshop on Smart Antennas (WSA 2014)*, Mar. 2014.

[12] O. De Candido, L. G. Baltar, A. Mezghani, and J. A. Nossek, "SIMO/MISO MSE-Duality for Multi-User FBMC for Highly Frequency Selective Channels," in *Proc. International ITG Workshop on Smart Antennas (WSA 2015)*, Mar. 2015.

[13] L. G. Baltar, M. Newinger, and J. A. Nossek, "Structured subchannel impulse response estimation for Filter Bank based Multicarrier systems," in *Proc. ISWCS 2012*, Aug. 2012.

[14] M. Sadek, A. Tarighat, and A. Sayed, "A Leakage-Based Precoding Scheme for Downlink Multi-User MIMO Channels," *IEEE Trans. Wireless Commun.*, vol. 6, no. 5, pp. 1711 – 1721, May 2007.

[15] M. Haardt, C. F. Mecklenbräuker, M. Vollmer, and P. Slanina, "Smart antennas for UTRA TDD," *European Transactions on Telecommunications (ETT)*, vol. 12, pp. 393 – 406, Sept.-Oct. 2001.

ISBN 978-3-8007-3662-1